Congress on Numerical Methods in Engineering
3–5 July 2017, Valencia, Spain
© SEMNI, 2017

COMPUTATION OF THE C5G7 NEUTRON TRANSPORT BENCHMARK USING A SPHERICAL HARMONICS-NODAL COLLOCATION METHOD

Mª Teresa Capilla[1], César Talavera[1], Damián Ginestar[1] and Gumersindo Verdú[2]

1: Departamento de Matemática Aplicada
Universitat Politècnica de València
Camino de Vera 14, 46022 Valencia, Spain
e-mail: {tcapilla,talavera,dginesta}@mat.upv.es

2: Departamento de Ingeniería Química y Nuclear
Universitat Politècnica de València
Camino de Vera 14, 46022 Valencia, Spain
e-mail: gverdu@iqn.upv.es

Keywords: Multi-dimensional P_L equations; spherical harmonics; nodal collocation method; two-dimensional C5G7 benchmark.

Abstract *The spherical harmonics method is applied to the angular dependence of the neutron transport equation, obtaining a finite approximation known as the P_L equations, that are rewritten as a vector-valued second order differential equation. Marshak vacuum boundary conditions are also considered. We have developed a nodal collocation method to spatially discretize the multi-dimensional P_L equations, for arbitrary odd order L, on a rectilinear mesh, based on the expansion of the neutronic fluxes in terms of orthonormal Legendre polynomials. In this work, the capability of the method to treat advanced reactor problems is verified with the 2D C5G7 MOX Fuel Assembly Benchmark, that is a criticality calculation proposed by NEA/NSC for testing the ability of modern deterministic transport methods and codes to treat heterogeneous reactor core problems without spatial homogenization. The large sparse generalized eigenvalue problem that arises is numerically solved on parallel computers using the software library SLEPc. The solution of this problem is obtained for different types of spatial meshes, for various P_L expansion orders and for different Legendre polynomial orders. We show that our results are consistent with the reference Monte Carlo solution.*

1 INTRODUCTION

The physical phenomena of neutron transport arises in a wide variety of fields in physics and engineering, such as nuclear reactors, nuclear medicine, radiological protection, etc. The neutron transport equation, which is a balance equation in a space of seven dimensions, mathematically describes these processes. Modern numerical approaches to this equation use Monte Carlo methods [1] or discrete-ordinates methods [2].

Monte Carlo methods model the nuclear system (almost) exactly and then solve the exact model statistically (approximately) anywhere in the modeled system. Because of its statistical nature, Monte Carlo core calculations usually involve a considerable computer time to attain reliable converged results. Discrete-ordinate methods are based on considering a finite set of angular directions and their corresponding weights that define an appropriate quadrature set in the unit sphere [3]. The main drawback of this kind of methods is that they suffer of ray effects, that is, they provide non-physical solutions for certain configurations.

Both kind of methods are very expensive from the computational point of view. To solve this problem, several approximations have been introduced to simplify the neutron transport equation. The usual approximation of the diffusion theory model allows a simple treatment of neutron transport in many realistic problems. With the advent of more complicated reactor core designs and the analysis of complex fuel assemblies in fine mesh applications, the diffusion equation does not provide good results.

A classical approach to solve the neutron transport equation is to apply the spherical harmonics method to the angular dependence of the equation, obtaining a finite approximation known as the P_L equations [4]. An advantage of the spherical harmonics method is that the equations are invariant under rotation of the coordinates and do not depend on the direction of the coordinates that should give no ray effects. The P_L equations are complicated and need a particular treatment. Simplified P_L approximations have been proposed [5], which can be easily implemented using essentially the same numerical methods as the ones used for the diffusion equation.

In Section 2, the spherical harmonics method, when applied to criticality calculations of the neutron transport equation, is briefly reviewed. The angular dependence of the equation is approximated by a finite set of equations known as the P_L equation, for arbitrary odd order L, that are then rewritten in a diffusive form as a vector-valued second order differential equation. Vacuum and reflective boundary conditions are also approximated using the spherical harmonics method. The spatial dependence of the multi-dimensional P_L equations is then discretized on a rectilinear mesh using a nodal collocation method, previously developed in [6, 7, 8], and based on the expansion of the neutronic fluxes in terms of orthonormal Legendre polynomials. In previous works [6, 7, 8] the method was validated for some 2D and 3D neutron transport benchmark problems. This procedure replaces the transport equation eigenvalue problem by an algebraic generalized eigenvalue problem.

To test the capability of the nodal collocation method to treat advanced reactor problems, in Section 3, we consider the 2D C5G7 MOX Fuel Assembly Benchmark, proposed in [9], for testing the ability of modern deterministic transport methods and codes to treat reactor heterogeneous core problems without spatial homogenization. Direct whole-core calculations are

computationally expensive and require massively parallel computing platforms and vast memory and disk space capabilities. The eigenvalue problem that arises from the application of the nodal collocation method to the C5G7 benchmark problem is numerically solved using SLEPc, a software library [10] for the solution of large scale sparse eigenvalue problems on parallel computers, that is based on the PETSc [11] data structures. We study the convergence of the solution of this problem with the order of the P_L approximation, and also with the Legendre polynomial order. We also analyze the results obtained with different types of spatial meshes.

2 THE TRANSPORT EQUATION AND THE P_L EQUATIONS

The physical phenomena of the neutron transport and interactions in the reactor core are modelled by the Boltzmann transport equation [12], that is a balance equation between neutrons lost by transport and absorption, produced or lost by scattering and produced by fission. Of particular relevance are *criticality calculations*. Physically, a system containing fissionable material is said to be critical if there is a self-sustaining time-independent chain reaction in the absence of external source of neutrons. Criticality calculations are normally cast into the form of eigenvalue problems:

$$\vec{\Omega}\,\vec{\nabla}\Phi(\vec{r},\vec{\Omega},E)+\Sigma_t(\vec{r},E)\,\Phi(\vec{r},\vec{\Omega},E)=Q_s(\vec{r},\vec{\Omega},E)+\frac{1}{\lambda}Q_f(\vec{r},\vec{\Omega},E)\,,\quad \vec{r}\in V\,, \tag{1}$$

with appropriate boundary conditions, for example, vacuum boundary conditions

$$\Phi(\vec{r},\vec{\Omega},E)=0\,,\quad \text{for all } \vec{\Omega}\,\vec{r}\leq 0, \text{ when } \vec{r}\in\partial V\,, \tag{2}$$

where ∂V is the boundary of the reactor volume V. Here $\Phi(\vec{r},\vec{\Omega},E)$ is the neutron angular flux at location $\vec{r}$ in the direction $\vec{\Omega}$ at time t; the position vector $\vec{r}=(x_1,x_2,x_3)$ is given in Cartesian coordinates; $\vec{\Omega}=(\cos\varphi\,\sin\theta\,,\,\sin\varphi\,\sin\theta\,,\,\cos\theta)$ is the direction, $0<\varphi<2\pi$, $0<\theta<\pi$; E is the neutron energy; Σ_t is the total macroscopic cross-section and Q_s and Q_f are the scattering source term and the source of neutrons by fission term respectively, given by

$$Q_s(\vec{r},\vec{\Omega},E,t)=\int dE'\int d\vec{\Omega}'\,\Sigma_s(\vec{r};\vec{\Omega}',E'\rightarrow\vec{\Omega},E)\,\Phi(\vec{r},\vec{\Omega}',E')\,,$$
$$Q_f(\vec{r},\vec{\Omega},E,t)=\frac{\chi_p(E)}{4\pi}\int dE'\,\nu\Sigma_f(\vec{r},E')\int d\vec{\Omega}'\,\Phi(\vec{r},\vec{\Omega}',E')\,,$$

where Σ_s is the scattering cross-section from $(\vec{\Omega}',E')$ to $(\vec{\Omega},E)$; Σ_f is the fission cross-section; ν is the average number of neutrons per fission and χ_p is the spectrum. A criticality calculation finds the largest value of λ for which a nonnegative fundamental mode solution exists, so $k_{\text{eff}}=\lambda_{\max}$.

The first approximation to numerically solve Eq. (1) is to replace the continuous variable E by a discretization into a finite number of energy groups $g\in G$, where group g spans the range of energies from E_g to E_{g+1}. This is known as the *energy multi-group approximation*. In order to facilitate the notation we will consider only the monoenergetic version of these equations, that is, one energy group.

2.1 The spherical harmonics method

In the spherical harmonics method the angular dependence of the neutronic flux $\Phi(\vec{r},\vec{\Omega})$ is expanded in terms of the (complex) spherical harmonics $Y_l^m(\vec{\Omega}) = H_l^m\, P_l^m(\cos\theta)e^{im\varphi}$, where $P_l^m(\cos\theta)$ are the associated Legendre polynomials and $H_l^m = \sqrt{\frac{(2l+1)}{4\pi}\frac{(l-m)!}{(l+m)!}}$, that form a complete set of orthonormal functions. Thus,

$$\Phi(\vec{r},\vec{\Omega}) = \sum_{l=0}^{\infty}\sum_{m=-l}^{+l} \phi_{lm}(\vec{r})\, Y_l^m(\vec{\Omega})\,, \tag{3}$$

where $\phi_{lm}(\vec{r})$ are the (spherical harmonics) moments. We observe that the transport equation (1) is a real equation and, as we are interested (for physical reasons) on real solutions, then $\Phi = \Phi^*$, that is, ${\phi_{lm}}^* = (-1)^m\phi_{l,-m}$ so there are only $2l+1$ real independent moments for each $l > 0$, that is, $\{\phi_{l0}, \mathrm{Re}\,\phi_{lm}, \mathrm{Im}\,\phi_{lm}, m = 1,\dots,l\}$.
It will also be assumed that scattering depends only on the relative angle between the incident and the scattered neutrons, $\vec{\Omega}\,\vec{\Omega}'$, and that the scattering cross-section may be expanded as the following series of Legendre polynomials:

$$\Sigma_s(\vec{r},\vec{\Omega}\,\vec{\Omega}') = \sum_{l=0}^{\infty}\frac{2l+1}{4\pi}\Sigma_{s,l}(\vec{r})\, P_l(\vec{\Omega}\,\vec{\Omega}')\,. \tag{4}$$

Expansions (3) and (4) and the orthogonality properties of Y_l^m are then used into Eq. (1). From these expressions it can be obtained the following (infinite) set of (complex) equations for the spherical harmonics moments ϕ_{lm} [8]:

$$\begin{aligned}
&\frac{1}{2}\Big(-C_1(l+1,m+1)\frac{\partial\phi_{l+1,m+1}}{\partial x_1} + C_2(l,m)\frac{\partial\phi_{l-1,m+1}}{\partial x_1}\\
&\qquad - C_1(l,m)\frac{\partial\phi_{l-1,m-1}}{\partial x_1} + C_2(l+1,m-1)\frac{\partial\phi_{l+1,m-1}}{\partial x_1}\Big)\\
&+\frac{1}{2i}\Big(-C_1(l+1,m+1)\frac{\partial\phi_{l+1,m+1}}{\partial x_2} + C_2(l,m)\frac{\partial\phi_{l-1,m+1}}{\partial x_2}\\
&\qquad - C_1(l,m)\frac{\partial\phi_{l-1,m-1}}{\partial x_2} + C_2(l+1,m-1)\frac{\partial\phi_{l+1,m-1}}{\partial x_2}\Big)\\
&+C_3(l+1,m)\frac{\partial\phi_{l+1,m}}{\partial x_3} + C_3(l,m)\frac{\partial\phi_{l-1,m}}{\partial x_3} + \Sigma_t\,\phi_{lm}\\
&\quad = \Sigma_{s,l}\,\phi_{lm} + \delta_{l0}\delta_{m0}\,\frac{1}{\lambda}\nu\Sigma_f\,\phi_{00}\,, \qquad l = 0,1,\dots\,, \quad m = -l,\dots,+l\,,
\end{aligned} \tag{5}$$

($C_j(l,m)$ are numerical coefficients). It is understood that terms involving moments ϕ_{lm} with invalid indices l and m are zero. To obtain a finite approximation, the series in expansions (3) and (4) are truncated at some finite order $l = L$ and the resulting Eqs. (5) are known as the (complex) P_L *equations*. In the following, we will only consider L to be an *odd integer*.

If we take real and imaginary part in Eqs. (5) and define the real moments

$$\begin{aligned} \xi_{lm} &= \mathrm{Re}\,\phi_{lm} = \frac{1}{2}(\phi_{lm} + (-1)^m \phi_{l,-m})\,, \\ \eta_{lm} &= \mathrm{Im}\,\phi_{lm} = \frac{1}{2i}(\phi_{lm} - (-1)^m \phi_{l,-m})\,, \end{aligned} \tag{6}$$

we can easily obtain the real form of P_L equations.
From the index structure of Eqs. (5) it is convenient to gather even l moments into vectors $X = (\xi_{l,m\geq 0}, \eta_{l,m>0})_{l=\text{even}}$, with $n_e = L(L+1)/2$ components, and odd l moments into vectors $\bar{X} = (\xi_{l,m\geq 0}, \eta_{l,m>0})_{l=\text{odd}}$, with $n_o = (L+1)(L+2)/2$ components (for example, if $L = 1$ then $X = (\xi_{00})$ and $\bar{X} = (\xi_{10}, \xi_{11}, \eta_{11})^T$). Then the real form of P_L equations (5) can be rewritten as

$$\sum_{j=1}^{3} M_j \frac{\partial \bar{X}}{\partial x_j} + \Sigma_a\, X = \frac{1}{\lambda}\,\mathrm{diag}(\delta_{l0}\,\nu\Sigma_f)_{l=\text{even}}\, X\,, \tag{7}$$

$$\bar{X} = -D \sum_{j=1}^{3} \bar{M}_j \frac{\partial X}{\partial x_j}\,, \tag{8}$$

where $\Sigma_a = \mathrm{diag}(\Sigma_t - \Sigma_{sl})_{l=\text{even}}$, $\bar{\Sigma}_a = \mathrm{diag}(\Sigma_t - \Sigma_{sl})_{l=\text{odd}}$, $D = \bar{\Sigma}_a^{-1} = \mathrm{diag}(\Sigma_t - \Sigma_{sl})^{-1}_{l=\text{odd}}$ is a square matrix, and M_j and $\bar{M}_j$ are rectangular matrices (of dimension $n_e \times n_o$ and $n_o \times n_e$, respectively) defined from the coefficients of Eqs. (5). Eq. (8) corresponds to a generalization of *Fick's law*. Replacing Eq. (8) into Eq. (7) we obtain the *diffusive form of P_L equations*

$$-\sum_{i,j=1}^{3} \frac{\partial}{\partial x_i}\left(M_i D \bar{M}_j \frac{\partial X}{\partial x_j}\right) + \Sigma_a X = \frac{1}{\lambda}\,\mathrm{diag}(\delta_{l0}\,\nu\Sigma_f)_{l=\text{even}} X\,. \tag{9}$$

The (square) *effective diffusion matrices* $M_i D \bar{M}_j$ generalize the diffusion coefficient $1/(3(\Sigma_t - \Sigma_{s1}))$ of P_1 equation to P_L equations for $L > 1$.
Finally, Eq. (9) corresponds to 3D geometry. Lower dimensional geometries are obtained by imposing restrictions to the angular neutronic flux. The XY (2D) geometry describes a medium with cross-sections and source independent of Z direction and can be obtained by imposing that the angular neutronic flux does not depend on the third coordinate, $\Phi = \Phi(x, y, \vec{\Omega})$, so $\frac{\partial \Phi}{\partial z} = 0$, and also must satisfy the symmetry relation $\Phi(\theta) = \Phi(\pi - \theta)$, so the moments $\phi_{lm} = 0$ if $l + m$ is odd. The planar (1D) geometry describes a medium that is transversely infinite (in the XY plane) with cross-section and source variation only in the Z direction; this case is obtained imposing that the neutronic flux $\Phi = \Phi(z, \theta)$ so the only nonzero moments are $\phi_{l,m=0} = \xi_{l0}$ and they are real.

2.2 Interface conditions

At points where the source or any cross-section is discontinuous, Eqs. (7) and (8) are undefined, and we will require some sort of interface conditions for these regions [13]. Let us replace the interface with a very thin transition region, where the physical properties of the medium

change rapidly, but continuously. If, for example, the discontinuity occurs at a YZ plane with coordinate $x_1 = x_{1,0}$, the transition region extends from $x_{1,0} - \Delta$ to $x_{1,0} + \Delta$. On integrating the P_L equations (7) and (8) over the transition region, we arrive at the following *interface conditions*

$$\lim_{\Delta \to 0+} M_1 \, \bar{X}(x_{1,0} + \Delta) = \lim_{\Delta \to 0+} M_1 \, \bar{X}(x_{1,0} - \Delta) \, , \tag{10}$$

$$\lim_{\Delta \to 0+} \bar{M}_1 \, X(x_{1,0} + \Delta) = \lim_{\Delta \to 0+} \bar{M}_1 \, X(x_{1,0} - \Delta) \, . \tag{11}$$

But matrix $\bar{M}_1$, of dimension $n_o \times n_e$ (with $n_o > n_e$ for odd L approximation) has rank n_e, so the second equation implies continuity of even order moments X at the interface,

$$\lim_{\Delta \to 0+} X(x_{1,0} + \Delta) = \lim_{\Delta \to 0+} X(x_{1,0} - \Delta) \, . \tag{12}$$

On the other hand, as $\dim(M_1) = n_e \times n_o$, the first equation gives n_e linear relations between the n_o ($> n_e$) odd moments $\bar{X}$, so it is not possible to impose continuity of *all* the moments.

2.3 Boundary conditions

Vacuum boundary conditions as given by Eq. (2) can be approximated by setting Marshak's conditions [12]

$$\int_{\vec{\Omega}\,\vec{n} \leq 0} d\vec{\Omega} \; Y_l^{m*}(\vec{\Omega}) \, \Phi(\vec{r}, \vec{\Omega}) = 0 \, , \tag{13}$$

for $l = 1, 3, 5, \ldots, L$ (odd) and $m = 0, 1, \ldots, l$. Notice that (13) is complex so there are $2l + 1$ real conditions for each odd index l.
We will only consider regions with prismatic geometry where we can use the symmetry $Y_l^m(-\vec{\Omega}) = (-1)^l Y_l^m(\vec{\Omega})$. Inserting the expansion given by the equation (3) into Marshak's conditions (13), it results into the conditions

$$\frac{1}{2}\phi_{lm} + \sum_{\substack{l' \text{ even} \\ -l' \leq m' \leq l'}}^{L-1} \Big(\int_{\vec{\Omega}\,\vec{n} \leq 0} d\vec{\Omega} \; Y_l^{m*}(\vec{\Omega}) \, Y_{l'}^{m'}(\vec{\Omega}) \Big) \phi_{l'm'} = 0 \, , \tag{14}$$

for $l = 1, 3, 5, \ldots, L$ and $m = 0, 1, \ldots, l$. Taking real and imaginary part in (14), Marshak's conditions can be written as

$$\bar{X} + N \, X = 0 \, , \tag{15}$$

where real vectors X and $\bar{X}$ were previously defined and N is a real rectangular matrix (of dimensions $n_o \times n_e$) with elements

$$N_{(lm),(l'm')} = 2 \int_{\vec{\Omega}\,\vec{n} \leq 0} d\vec{\Omega} \; Y_l^{m*}(\vec{\Omega}) \, Y_{l'}^{m'}(\vec{\Omega})$$

((lm), l odd, are row indices; $(l'm')$, l' even, are column indices, with appropriate ordering), whose numerical values depend on the geometry of the boundary surface, that is, the spatial axis normal to the boundary surface.

Notice that Marshak's conditions (15) depend on the order L of the angular approximation and form a system of n_o linear equations. We treat the discontinuity between the external surface and the interior region by inserting a very thin transition region. If, for example, the boundary surface has normal vector $\vec{n}$ pointing to X axis and is located at $x_1 = x_{1,0}$, the transition region covers the interval $[x_{1,0}, x_{1,0} + \Delta]$. We obtain the following interface conditions:

$$\lim_{\Delta \to 0+} M_1 \, \bar{X}(x_{1,0} + \Delta) = M_1 \, \bar{X}(x_{1,0}) \qquad \text{and} \qquad \lim_{\Delta \to 0+} X(x_{1,0} + \Delta) = X(x_{1,0}) \, , \tag{16}$$

so X is continuous at the interface but, using Eq. (15), $\bar{X}$ satisfies the interface condition

$$\lim_{\Delta \to 0+} M_1 \, \bar{X}(x_{1,0} + \Delta) = -M_1 \, N \, X(x_{1,0}) \, , \tag{17}$$

that is, a system of n_e linear conditions.
Reflective boundary conditions are applied at planes of symmetry. If physical conditions are equal at both sides, the neutronic flux must satisfy, at the symmetry plane, $\Phi(\vec{r}, \vec{\Omega}) = \Phi(\vec{r}, \vec{\tilde{\Omega}})$, where $\vec{\tilde{\Omega}}$ is the reflected angular direction with respect to the symmetry plane. For example, if the normal vector $\vec{n}$ to the symmetry plane points to the negative Z axis, the symmetry condition is

$$\Phi(\vec{r}, \varphi, \theta) = \Phi(\vec{r}, \varphi, \pi - \theta) \, , \quad \text{for } 0 < \varphi < 2\pi \, , \; 0 < \theta < \pi/2 \, . \tag{18}$$

Inserting expansion (3), this equation is equivalent to the following

$$\sum_{l=0}^{\infty} \sum_{m=-l}^{+l} (1 - (-1)^{l+m}) \, \phi_{lm}(\vec{r}) \, Y_l^m(\vec{\Omega}) = 0 \, ,$$

that is,

$$\phi_{lm} = 0 \, , \qquad \text{whenever } l + m \text{ odd} \quad (l = 0, 1, \ldots \, ; \; m = 0, 1, \ldots, l) \, . \tag{19}$$

2.4 The nodal collocation method

Since P_L equations (9) have a diffusive form, their spatial discretization can be done using a nodal collocation method, previously used for the neutron diffusion equation [14, 15] and generalized for eigenvalue problems in multi-dimensional rectangular geometries in [6, 7, 8].
Given a rectilinear mesh with vertex coordinates $\{x_{1,i_1}, x_{2,i_2}, x_{3,i_3}\}$, where $i_j = 0, 1, \ldots, m_j$ $(j = 1, 2, 3)$ are vertex indices, the spatial domain is discretized into N $(\leq m_1 \times m_2 \times m_3)$ adjacent rectangular prisms, or nodes, of the form $N^e = [x_{1,i_1}, x_{1,i_1+1}] \times [x_{2,i_2}, x_{2,i_2+1}] \times [x_{3,i_3}, x_{3,i_3+1}]$, being $e = 1, \ldots, N$ the index that enumerates the nodes, once an appropriate node ordering has been chosen, see Fig. 1. The nodal collocation method assumes that on each node N^e the cross-sections in Eq. (1) are constant.
The change of variables $u_j = \frac{1}{\Delta x_j^e} \Big(x_j - \frac{1}{2}(x_{j,i_j} + x_{j,i_j+1}) \Big)$, $j = 1, 2, 3$, where $\Delta x_j^e = x_{j,i_j+1} - x_{j,i_j}$, transforms the node N^e into the cubic node of volume one $N_u^e = [-\frac{1}{2}, +\frac{1}{2}]^3$. For each node N_u^e, it is assumed that the spatial dependence of vector $X^e(u_1, u_2, u_3)$ of l even moments

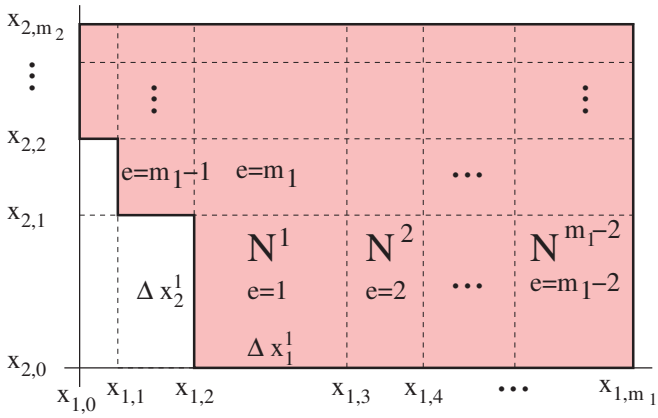

Figure 1: Sample rectilinear mesh covering the domain for 2D geometry. A *natural* ordering for spatial nodes N^e has been chosen.

(defined in Eq. (9)) can be expanded in terms of (orthonormal) Legendre polynomials $\mathcal{P}_k(u)$ [6] up to a certain finite order M,

$$X^e(u_1,u_2,u_3) = \sum_{k_1,k_2,k_3=0}^{M} x^e_{k_1k_2k_3} \mathcal{P}_{k_1}(u_1)\,\mathcal{P}_{k_2}(u_2)\,\mathcal{P}_{k_2}(u_3)\,, \tag{20}$$

where the Legendre coefficients $x^e_{k_1k_2k_3}$ are the unknowns to be determined. The series (20) is then inserted into Eqs. (9) and equations for the Legendre moments $x^e_{k_1k_2k_3}$ are derived multiplying by the weight function $W_{r_1r_2r_3} = \mathcal{P}_{r_1}(u_1)\,\mathcal{P}_{r_2}(u_2)\,\mathcal{P}_{r_3}(u_3)$, $r_1, r_2, r_3 = 0, 1, \ldots, M$, and integrating over the cube N^e_u.
In performing this process, integration of "diagonal terms" in Eqs. (9), that is, $\Sigma_a\, X^e$ and $\mathrm{diag}(\delta_{l0}\,\nu\Sigma_f)_{l=\text{even}} X^e$, is straightforward using the orthonormality properties of $\mathcal{P}_k(u)$.
Double derivative terms in Eqs. (9) involve coupling with neighbouring nodes using interface conditions. If node N^e_u is an interior node and, for example, the boundary between two adjacent nodes falls in the YZ plane, with normal vector to the surface pointing to the negative X axis, adjacent nodes are then related imposing $(2 \times n_e)$ *interface conditions* given by Eqs. (10) and (12),

$$X^e(u_1 = -\frac{1}{2}, u_2, u_3) \;=\; X^{e_1}(u_1 = +\frac{1}{2}, u_2, u_3)\,, \tag{21}$$

$$M_1\,\bar{X}^e(u_1 = -\frac{1}{2}, u_2, u_3) \;=\; M_1\,\bar{X}^{e_1}(u_1 = +\frac{1}{2}, u_2, u_3)\,. \tag{22}$$

In the case that the node N^e_u is adjacent to the vacuum boundary as, for example, when the vacuum boundary falls in the XY plane and the normal vector to the surface points to the negative Z axis, then Marshak vacuum boundary conditions and interface conditions (17) are used,

$$M_3\,\bar{X}^e\big(u_1,u_2,-\frac{1}{2}\big) = -M_3\,N_3^-\,X^e\big(u_1,u_2,-\frac{1}{2}\big)\,. \tag{23}$$

Finally, once an appropriate ordering of the indices is chosen, the previous procedure approximates Eqs. (9) by a generalized eigenvalue problem

$$\mathcal{A}\,V = \frac{1}{\lambda}\mathcal{B}\,V\ , \tag{24}$$

where V is a real vector of components $(\xi^{m;e}_{l;k_1k_2k_3}, \eta^{m;e}_{l;k_1k_2k_3})$ and $\mathcal{A}$, $\mathcal{B}$ are matrices of dimension

$$N \times G \times N_{\text{Leg}} \times n_e\ , \tag{25}$$

where N is the number of nodes; G is the number of energy groups; $N_{\text{Leg}} = M^d$ is the number of Legendre moments, with M the order in Legendre series (20) and d the spatial dimension and finally $n_e = L(L+1)/2$ is the number of components of vector X (i.e. the number of even l moments), being L the order of the P_L approximation.

3 CALCULATION OF THE SEVEN-GROUP 2D C5G7 BENCHMARK

The spherical harmonics-nodal collocation method described in the previous sections has been implemented into the multi-group multi-dimensional code SHNC (Spherical Harmonic-Nodal Collocation) written in FORTRAN 90. The SHNC code computes and solves the discretized generalized real non-symmetric eigenvalue problem (24), that is formulated as $\mathcal{B}\,V = \lambda\,\mathcal{A}\,V$, where $\mathcal{A}$, $\mathcal{B}$ are large and sparse matrices, for an arbitrary P_L approximation, with odd L. The largest eigenvalue $\lambda \in \mathbb{R}$ is effectively computed on parallel computers using the software library SLEPc [10], that is based on the PETSc [11] data structures and employs the MPI standard. The perfomance of the code and the accuracy and convergence of the method have been already tested in previous works [6, 7, 8], with several eigenvalue problems in multi-dimensional geometries.

In this work, we analize the application of the SHNC code to calculate the two-dimensional C5G7 fuel assembly benchmark. The Nuclear Energy Agency (NEA) of the Organization for Economic Cooperation and Development (OECD) proposed the C5G7 benchmark to test the ability of modern deterministic transport methods to treat reactor heterogeneous core problems without spatial homogenization [9]. This benchmark problem has been analyzed with various code packages [9], and a reference solution was obtained using the Monte Carlo code, providing the k_{eff} eigenvalue solution, and also the core pin power predictions.

Now we present the P_L results of the 2D C5G7 benchmark obtained with SHNC, in order to study the convergence and accuracy of the SHNC P_L solutions. The P_L results will be compared with the reference MCNP solutions [9]. For all computations, a Krylov-Schur method was chosen as eigensolver and linear systems were iterative solved with the biconjugate gradient stabilized (BCGs) method using HYPRE BoomerAMG as parallel preconditioner. Computational times vary from some hours to a few days on a Xeon CPU E5-2650 using 8 cores.

The configuration of the 2D C5G7 MOX benchmark consists of a core with two MOX and two UO_2 fuel assemblies surrounded by a moderator region, as it is shown in Fig. 2(a) for the quarter core. Vacuum boundary conditions are applied to the right and to the bottom boundaries, and reflective conditions to the top and to the left boundaries. Each fuel assembly consists of

17×17 lattice of square fuel pin cells, the geometry and composition of a fuel pin cell can be seen Fig. 2(b). Every fuel pin cell consists of a single moderator region outside a circular region (fuel-clad mix) representing a fuel pin, a fission chamber or a guide tube. The same moderator composition is used in all the fuel pin cells and in the water reflector (moderator) surrounding the assemblies (see Fig. 2(a))

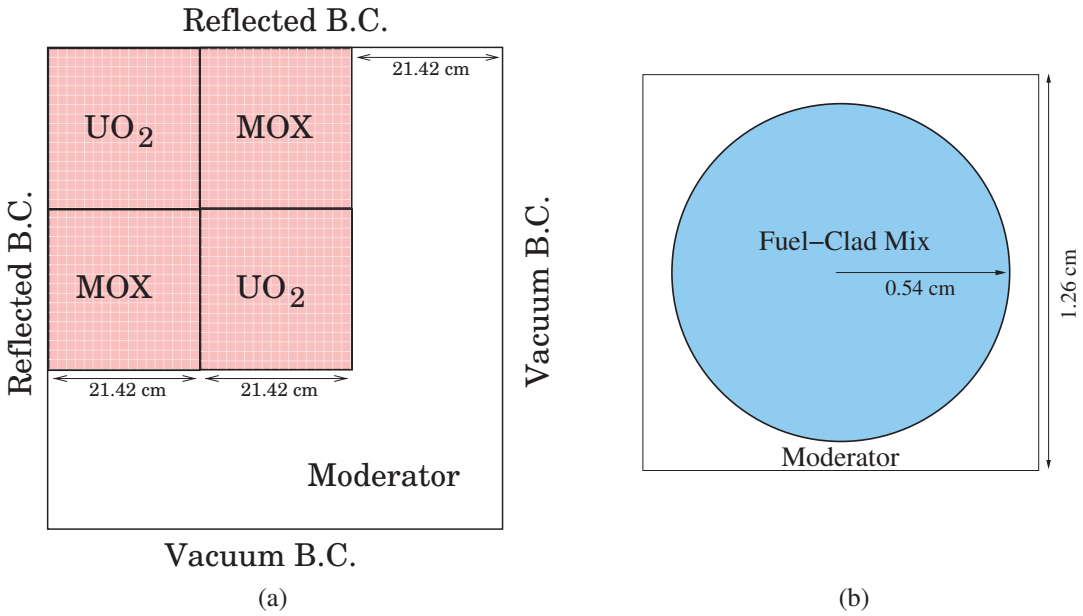

Figure 2: (a) The core configuration for the 2D C5G7 benchmark problem, and (b) a fuel pin cell geometry showing regions of fuel and moderator.

More details about the fuel pin cell compositions and the seven-group isotropic scattering cross-sections for UO_2, MOX, the guide tubes, fission chamber and the moderator are provided in [9]. To calculate the solution of the C5G7 benchmark with SHNC, two different types of mesh discretizations of the pin cells were used, both preserving the circular region area. Fig. 3(a) shows the rectangular mesh type A, with 6×6 cartesian nodes per lattice pin cell. Fig. 3(b) shows a finer level of spatial resolution, the mesh type B, with the pin cell divided into 7×7 nodes.

Also, for each type of mesh discretization, A and B, we have used two different models corresponding to different levels of spatial resolution for the moderator region extended to the right and bellow the outer assemblies.

The discretization with meshes type A and B for the pin cells, were continued for every cell in the moderator region, giving a calculation with a total of $306 \times 306 = 93636$ 2D spatial nodes for mesh A and $357 \times 357 = 127449$ nodes for mesh B, named as meshes A1 and B1, respectively.

Another spatial discretization was then considered for the moderator region, that is schematically described in Fig. 4 for mesh type B, and taken in a similar way for mesh type A. These

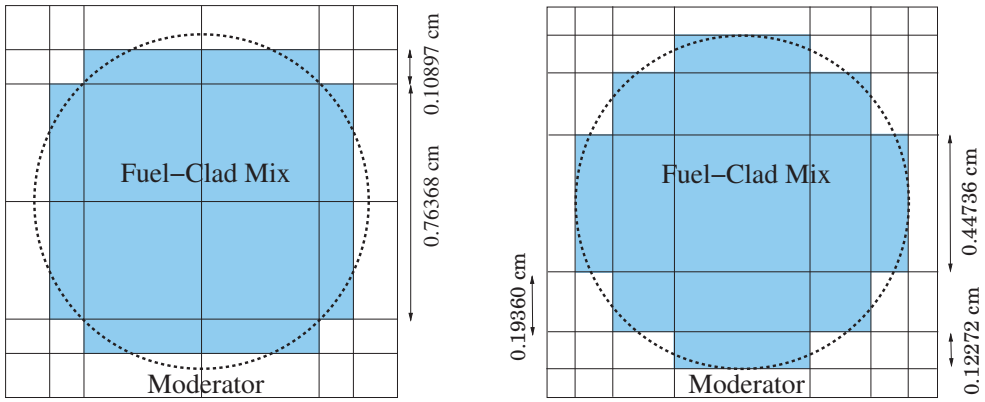

Figure 3: (a) Mesh A: SHNC spatial discretization by a 6×6 nodes, and (b) Mesh B: spatial discretization by a 7×7 nodes.

models are named as A2 and B2. The highly anisotropic behavior of the flux is localized in the vicinities of MOX assemblies. Then, in order to obtain a smooth transition, the fuel region nodalisation was continued for the first 6 neighbouring cells in the moderator (see Fig. 4). Then, meshes A1 and A2 allow us to obtain a reference P_L solution. As meshes A2 and B2 give about a 34% reduction in the number of nodes, we will check if there is loss of precision in the results with this reduction.

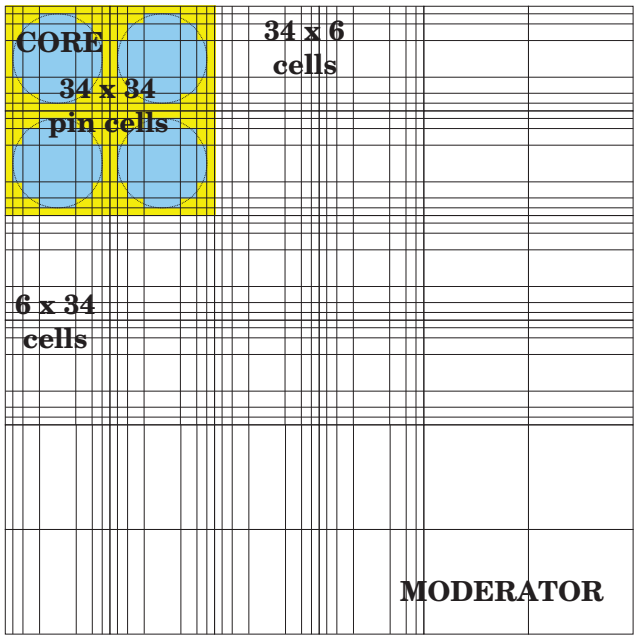

Figure 4: Schematic description of B2 mesh, showing the grid of the moderator region.

The numerical P_L results using each type of mesh were calculated with different Legendre polynomial order (Eq. (20), $M = 3$ and $M = 4$). Table 1 shows the k_{eff} eigenvalue solutions obtained with the P_L approximations and percent relative errors with respect to the reference MCNP solution, defined as $100(k_{\text{eff}}^{\text{SHNC}} - k_{\text{eff}}^{\text{MCNP}})/k_{\text{eff}}^{\text{MCNP}}$. The statistical error for the reference MCNP solution in the Table is associated to the 98% confidence interval.

MCNP: $k_{\text{eff}} = 1.186550$ (± 0.008)					
SHNC	M	k_{eff} and percent error	SHNC	M	k_{eff} and percent error
Mesh A1			Mesh A2		
P_1	3	1.183922 (-0.221)	P_1	3	1.183700 (-0.240)
	4	1.183813 (-0.231)		4	1.183818 (-0.230)
P_3	3	1.180198 (-0.535)	P_3	3	1.180140 (-0.540)
	4	1.177268 (-0.782)		4	1.176693 (-0.830)
Mesh B1			Mesh B2		
P_1	3	1.183433 (-0.263)	P_1	3	1.183244 (-0.279)
	4	1.183056 (-0.294)		4	1.182943 (-0.304)
P_3	3	1.187656 ($+0.093$)	P_3	3	1.186949 ($+0.034$)
	4	1.183001 (-0.299)		4	1.181710 (-0.408)

Table 1: k_{eff} eigenvalue solutions and percent errors for the C5G7 benchmark, computed with different spatial meshes and values of M.

As there are a total of 1056 fuel pins in the four assemblies type MOX and UO_2, a direct comparison of the pin power results against the reference solution in each individual pin would be difficult. Therefore, several error measures were used in the form of average pin power percent error (AVG), root mean square (RMS) of the pin power percent error distribution and mean relative pin power percent error (MRE) [9]. In Table 2 we show the pin power distribution error measures for the P_1 and P_3 solutions obtained with the four types of meshes described above, for different values of the Legendre polynomial order M, together with the reference MCNP solution. We observe that the error measures of the P_L solutions decrease as the angular order L increases and in general, the decrease of the P_3 errors is greater when the order M is increased from 3 to 4.

Table 3 gives the values of the maximum and the minimum pin power obtained with SHNC, along with the percent errors with respect to the reference MCNP solutions.

The P_1, P_3 solutions for the MOX and UO_2 assembly powers, and the reference MCNP are shown in Table 4. The results shown in Tables 3 and 4 where calculated using the mesh A1, with 6×6 nodes per pin cell and Legendre polynomial order $M = 4$.

Figs. 5(a) and 5(b) display the contour maps of the P_3 fast (group 1) and thermal (group 2) scalar fluxes, respectively. For this calculation we used the B1 reference mesh and order $M = 4$.

		AVG	RMS	MRE
MCNP		0.32	0.34	0.27
SHNC	M	Mesh A1		
P_1	3	1.47	1.78	1.27
	4	1.48	1.78	1.28
P_3	3	0.89	1.04	0.88
	4	0.63	0.74	0.61
SHNC	M	Mesh B1		
P_1	3	1.44	1.75	1.22
	4	1.43	1.77	1.18
P_3	3	1.14	1.34	1.15
	4	0.85	1.00	0.84

Table 2: Pin power error measures for the 2D C5G7 benchmark.

	Maximum pin power	Percent error	Minimum pin power	Percent error	Maximum percent error
MCNP	2.498	± 0.16	0.232	± 0.58	
SHNC P_1	2.525	1.09	0.240	3.77	5.92
SHNC P_3	2.521	0.93	0.234	1.24	1.85

Table 3: Specific pin powers and percent error results for 2D C5G7 benchmark.

	Inner UO_2	Percent error	MOX	Percent error	Outer UO_2	Percent error
MCNP	492.8	± 0.10	211.7	± 0.18	139.8	± 0.20
SHNC P_1	496.0	0.65	210.6	-0.52	138.8	-0.72
SHNC P_3	495.5	0.54	210.5	-0.59	139.6	-0.10

Table 4: Assembly power and percent error results for 2D C5G7 benchmark.

4 CONCLUSIONS

We have studied the validity of the spherical harmonics-nodal collocation method to treat reactor heterogeneous core problems as the 2D C5G7 MOX Fuel Assembly Benchmark. Although the results are consistent with the reference solution, our eigenvalue results show oscillatory behaviour. Like any spectral method, P_L equations may suffer from highly oscillatory behaviour. This issue will be addressed in future works.

We also observe that the spatial approximation of the pin cell has less impact on the quality of the calculations than the angular modeling. There are no significant differences between the P_1 results with meshes type A and B, but results for k_{eff} with the P_3 approximation show

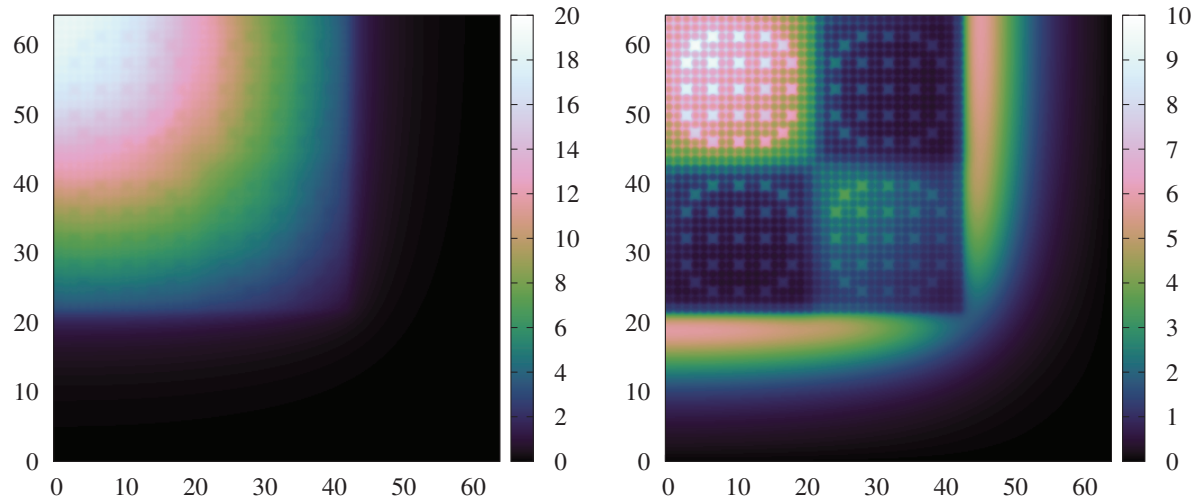

(a) P_5 scalar flux for Group 1

(b) P_5 scalar flux for Group 7

Figure 5: Contour plot of the P_3 fast (a) and thermal (b) flux distribution for C5G7 benchmark.

smaller errors when the spatial resolution is increased (meshes type B). We can conclude that the P_L k_{eff} eigenvalue solutions for mesh B are within the 98% confidence interval of the MCNP eigenvalue. Better computational efficiency is obtained with meshes A2 and B2, that maintain almost the same accuracy as the calculations with meshes A1 and B1, while the computational time and memory required for the calculations is about a 34% lower.

A decrease of the pin power and assembly power error measures with respect to MCNP is observed when the order L is increased. An advantadge of our method is that the pin power maximum percent error is lower than in classical deterministic methods; this error usually represents the largest deviations between Monte Carlo calculations.

From the above results, we conclude that the SHNC P_L approximation reproduces the power distribution and the scalar flux reasonably well, being able to obtain consistent solutions for typical reactor calculations, where P_1 and P_3 are practical approximations. The remaining errors can be attributed to the high-order space-angle approximation necessary to solve this particular benchmark problem.

REFERENCES

[1] J. Spanier and E.M. Gelbard, *Monte Carlo principles and neutron transport problems*, Dover Publications. Mineloa, NY, (2008).

[2] E.E. Lewis and W.F. Miller, *Computational methods of neutron transport*, American Nuclear Society. IL. USA, (1984).

[3] R. Sánchez and N.J. McCormick, "A review of neutron transport approximations", *Nucl. Sci. and Eng.*, Vol. **80**: pp.481-535, (1982).

[4] B. Davison, 1957. *Neutron Transport Theory*, Oxford University Press, London, (1957).

[5] E.M. Gelbard, *Spherical harmonics methods: P_L and double P_L approximations. Computing Methods in Reactor Physics*, Kelberg, D., Okrent, C. N. (eds.). Gordon and Breach, New York, (1968).

[6] M. Capilla, C.F. Talavera, D. Ginestar and G. Verdú, "A nodal collocation method for the calculation of the lambda modes of the P_L equations", *Ann. Nucl. Energ.*, Vol. **32**, pp. 1825-1853, (2005).

[7] M. Capilla, C.F. Talavera, D. Ginestar and G. Verdú, "A nodal collocation approximation for the multidimensional P_L equations - 2D applications", *Ann. Nucl. Energ.*, Vol. **35**, pp. 1820-1830, (2008).

[8] M. Capilla, C.F. Talavera, D. Ginestar, G. Verdú, "Application of a nodal collocation approximation for the multidimensional P_L equations to the 3D Takeda benchmark problems", *Ann. Nucl. Energ.*, Vol. **40**, pp. 1-13, (2012).

[9] NEA/NSC/DOC, 2003, 16, Nuclear Energy Agency, Organization for Economic Cooperation and Development, ISBN 92-64-02139-6 (2003).

[10] V. Hernández, J. E. Román and V. Vidal, "SLEPc: A scalable and flexible toolkit for the solution of eigenvalue problems", *ACM Trans. Math. Soft.*, Vol. **31**(3), pp. 351-362, (2005).

[11] S. Balay, S. Abhyankar, M. Adams, J. Brown, P. Brune, K. Buschelman, L. Dalcin, V. Eijkhout, W. Gropp, D. Karpeyev, D. Kaushik, M. Knepley, L.C. McInnes, K. Rupp, B. Smith, S. Zampini, H. Zhang, and H. Zhang, *PETSc Users Manual*, Technical Report ANL-95/11 - Revision 3.7, Argonne National Laboratory, (2016).

[12] W.M. Stacey, *Nuclear Reactor Physics*, Wiley, New York, (2001).

[13] H. Greenspan, C.N. Kelber and D. Okrent, *Computing Methods in Reactor Physics*, Gordon & Breach Science Publishers, New York, (1968).

[14] A. Hébert, "Development of the nodal collocation method for solving the neutron diffusion equation", *Ann. Nucl. Energ.*, Vol. **14**(10), pp. 527-541, (1987).

[15] G. Verdú, D. Ginestar, V. Vidal and J.L. Muñoz-Cobo, "3D λ modes of the neutron diffusion equation", *Ann. Nucl. Energ.*, Vol. **21**(7), pp. 405-421, (1994).